Pramāṇa, Vol. 6, No. 3, 1976, pp. 146–160. © Printed in India.

Alpha decay of isobaric analogue states in ^{24}Mg and ^{28}Si

AMIT ROY, M L JHINGAN and K V K IYENGAR
Tata Institute of Fundamental Research, Bombay 400005

MS received 28 July 1975; after revision 26 November 1975

Abstract. The α-decay of isobaric analogue states (which are forbidden by isospin selection rules) excited in ^{24}Mg and ^{28}Si through proton capture by ^{23}Na at E_p = 677 and 739 keV and by ^{27}Al at E_p = 295, 327 and 405 keV, respectively, have been studied using solid state track detectors. The ratio of α-decay widths of the two resonance states in ^{24}Mg to the state at 1·632 MeV (2^+) in ^{20}Ne yields the value 0·065 for the mixing parameter ϵ and the value 4·01 keV for the Coulomb matrix element responsible for the isospin mixing in ^{24}Mg.

In ^{28}Si the measurement of the α-decay widths of the three resonance states resulted in the determination of the proton, gamma and alpha partial widths which comprise the total width of the resonance states. Limits have been set for the value of the two mixing parameters involved in this case. Upper limits of 16 and 39 keV have been obtained for the Coulomb matrix elements responsible for the isospin mixing in ^{28}Si.

Keywords. Solid (plastic) state track detector; nuclear levels; resonance strengths; isobaric analogue states; Coulomb matrix element; isospin mixing parameter.

1. Introduction

Alpha decay of an isobaric analogue state (IAS) to low-lying states of the residual nucleus is isospin forbidden. Observation of alpha decay from such a state would therefore imply that the isospin of the state is not pure. It is the Coulomb interaction which is responsible for the mixing of states with different isospin. Let us suppose that the Coulomb force mixes the pure IAS with a compound nuclear state of lower isospin. This would result in two states with mixed isospin, which can be excited as resonances in a reaction. These are called the split components of an isobaric analogue resonance (IAR). The alpha decay widths from the split components would allow us to extract the value of the Coulomb matrix element responsible for the isospin mixing. The IAR can also mix with two states of lower isospin resulting in three split components of an IAR.

In the nucleus ^{24}Mg, two states at energies of 12·342 and 12·402 MeV have been excited as resonances at E_p = 677 and 739 keV, respectively in the ^{23}Na(p, γ) ^{24}Mg reaction (Endt and Van der Leun 1967, 1973). Both these states have been assigned $J^\pi = 3^+$ and their γ-decay branching ratios are almost identical (Meyer *et al* 1972). Thus these resonances are most likely to be components of an IAR. The IAS corresponding to the ground state of ^{24}Na occurs at 9·517 MeV in ^{24}Mg

(Endt and Van der Leun 1973). The states at 12·342 and 12·402 MeV are thus likely to be the split components of an IAR corresponding to the 2·909 MeV (3^+) state in ^{24}Na. Previous experiments using surface barrier detectors for detection of α's (Kuperus *et al* 1963) failed to measure any α-decay to the ground state of ^{20}Ne from these resonances. However, since these states have $J^\pi = 3^+$, no α-decay to the ground state of ^{20}Ne(0^+) will take place. Only α-decay to the 1st excited state of ^{20}Ne(2^+) at 1·632 MeV is energetically possible [Q (α-decay to 1·632 MeV) = 0·746 MeV]. The α-decay of the resonance at $E_p = 739$ keV to the 1·632 MeV state in ^{20}Ne has been observed by Meyer *et al* (1972) through the γ-deexcitation of that state.

We have measured the α-decay width for both the resonances at $E_p = 677$ and 739 keV employing solid state (plastic) track detector (SSTD).

Three states at 11·689, 11·898 and 11·974 MeV in ^{28}Si have been excited as resonances at $E_p = 295$, 327 and 405 keV respectively through the ^{27}Al(p, γ)^{28}Si reaction (Endt and Van der Leun 1967, 1973). The γ-decay of these resonances are found to be similar and take place predominantly to 4^+ states in ^{28}Si (Meyer *et al* 1969). All these resonances have been tentatively assigned $J^\pi = 4^+$. Since the IAS corresponding to the ground state of ^{28}Al occurs at 9·319 MeV in ^{28}Si (Endt and Van der Leun 1973), these resonances are likely to be split components of an IAR corresponding to the state at 2·66 MeV in ^{28}Al whose J^π is likely to be between 2^+ and -4^+ (Endt and Van der Leun 1973).

Kuperus *et al* (1963) studied the reaction ^{27}Al(p, α)^{24}Mg at these proton energies but failed to observe any α-decay from these resonances. In this case, although α-decay to both the ground state (0^+) ($Q\alpha_0 = 1·601$ MeV) and the 1st excited state at 1·368 MeV (2^+) ($Q\alpha_1 = 0·233$ MeV) in ^{24}Mg are energetically possible, the decay to the 1st excited state is inhibited by the extremely low α-penetrability.

In this study we have measured the α-decay from these three resonances using plastic track detectors.

2. Theory

The main quantity of interest in α-decay of a resonance is the decay width, Γ_α When only the proton, gamma and alpha channels are open for decay, as is the case in the present study, a knowledge of the resonance strengths of the (p, γ), (α, γ) and (p, α) reactions, will help determine the partial widths, Γ_p, Γ_γ and Γ_α which together constitute the total width, Γ. The resonance strengths are defined as $(2J+1)\frac{\Gamma_1\Gamma_2}{\Gamma}$ where J is the spin, Γ_1 and Γ_2 are partial widths and Γ the total width of the resonance state and the subscripts 1 and 2 refer to the incoming and outgoing channels. For situations where all the three resonance strengths are not known, further assumptions on the partial widths are necessary to extract their values from the resonance strengths.

Let us consider the α-decay of resonant states with mixed isospin. First we discuss the case of an IAS ($T = T_>$) mixing with a state of lower isospin ($T = T_< = T_> - 1$). The wave functions of the mixed states can be written as

$$\psi_1 = \frac{1}{\sqrt{1+|\epsilon|^2}}\{\psi(T_<) + \epsilon\psi(T_>)\} \tag{1}$$

$$\psi_2 = \frac{1}{\sqrt{1+|\epsilon|^2}}\{\psi(T_>) - \epsilon\psi(T_<)\} \tag{2}$$

where $\psi(T_<)$ and $\psi(T_>)$ are wave functions of the members with lower and higher isospin, respectively, of the unmixed doublet and ϵ is a complex mixing parameter. This mixing problem has been considered earlier by many workers (Radicati 1953, McDonald 1960) who treated ϵ as real. The complex nature of ϵ has been pointed out recently by Shanley (1975). The energy eigenvalues of ψ_1 and ψ_2 are given by

$$\eta_i = E_i - \frac{i}{2}\Gamma_i \tag{3}$$

where E_i are the resonance energies and Γ_i are the widths of the resonance. In the case of only one open channel, the phase of ϵ is given by the relation (Shanley 1975, Warke 1975)

$$\tan\phi_\epsilon = \frac{1+|\epsilon|^2}{1-|\epsilon|^2}\,\frac{\Gamma_2-\Gamma_1}{2(E_2-E_1)}. \tag{4}$$

The widths are given by

$$\frac{1}{2}\Gamma_i = \Sigma_f |\langle f | V | \psi_i \rangle|^2 \tag{5}$$

where f is the channel to which decay takes place and V is the decay operator. f is assumed to have pure isospin $T = T_<$ and V is assumed to conserve isospin. Then for α-decay from ψ_1 and ψ_2 only the $\psi(T_<)$ component would contribute, and thus

$$\frac{\Gamma_{\alpha_2}}{\Gamma_{\alpha_1}} = |\epsilon|^2. \tag{6}$$

Thus the ratio of the α-decay widths would determine the magnitude of the mixing parameter, ϵ.

Now, it is the Coulomb interaction, H_c, which is responsible for the mixing. Treating this mixing as a perturbation problem, the Coulomb matrix element non-diagonal in T, which is responsible for mixing can be written as (Warke 1975)

$$\langle \psi(T_<) | H_c | \psi(T_>)\rangle \approx \frac{\epsilon\cdot(\eta_1-\eta_2)}{1+|\epsilon|^2} \tag{7}$$

for small values of ϵ. In this case

$$\tan\phi_\epsilon \approx \frac{\Gamma_2-\Gamma_1}{2(E_\epsilon - E_1)}$$

and

$$\text{phase}\,(\eta_1-\eta_2) = \tan^{-1}\left\{\frac{\Gamma_2-\Gamma_1}{2(E_1-E_2)}\right\}.$$

Thus, for weak mixing, the phase of the product on the R.H.S. of eq. (7) is zero and the matrix element $\langle H_c\rangle$ is real.

We consider now the case of an IAS mixing with two states, say $\psi(T_<)$ and $\psi'(T_<)$ of lower isospin $T_<$ giving rise to three split components of an IAR. We can write, then

$$\psi_1 = \frac{1}{\sqrt{1+|\epsilon_1|^2}}\{\psi(T_<) + \epsilon_1\psi(T_>)\} \tag{8}$$

$$\psi_2 = \frac{1}{\sqrt{1+|\epsilon_2|^2}}\{\psi'(T_<) + \epsilon_2\psi(T_>)\} \tag{9}$$

$$\psi_3 = \frac{1}{\sqrt{1+|\epsilon_1|^2+|\epsilon_2|^2}}\{\psi(T_>) - \epsilon_1\psi(T_<) - \epsilon_2\psi'(T_<)\} \tag{10}$$

We assume here for ease of computation that the states $\psi(T_<)$ and $\psi'(T_<)$ are orthogonal. This assumption would give us upper bounds of isospin mixing. Using eq. (5) and the fact that α-decay takes place from $T_<$ components only, we find

$$\Gamma_{a_1} = \frac{1}{1+|\epsilon_1|^2}\Sigma_f |\langle f|V|\psi(T_<)\rangle|^2 \tag{11}$$

$$\Gamma_{a_2} = \frac{1}{1+|\epsilon_2|^2}\Sigma_f |\langle f|V|\psi'(T_<)\rangle|^2 \tag{12}$$

$$\Gamma_{a_3} = \frac{1}{1+|\epsilon_1|^2+|\epsilon_2|^2}\Sigma_f |\epsilon_1\langle f|V|\psi(T_<)\rangle + \epsilon_2\langle f|V|\psi'(T_<)\rangle|^2 \tag{13}$$

The final states f are assumed to have isospin $T = T_<$. Due to the presence of cross-terms in Γ_{a_3}, we find that the α-widths alone are not sufficient to determine the mixing parameters ϵ_1 and ϵ_2. However, it is possible to obtain the bounds on the magnitudes of the mixing parameters in this case. Let us define

$$A_f = \langle f|V|\psi(T_<)\rangle$$

and

$$B_f = \langle f|V|\psi'(T_<)\rangle.$$

Then eqs (11) to (13) become

$$\Gamma_{a_1} = \frac{1}{1+|\epsilon_1|^2}\Sigma_f |A_f|^2 \tag{14}$$

$$\Gamma_{a_2} = \frac{1}{1+|\epsilon_2|^2}\Sigma_f |B_f|^2 \tag{15}$$

$$\begin{aligned}\Gamma_{a_3} &= \frac{1}{1+|\epsilon_1|^2+|\epsilon_2|^2}\Sigma_f |\epsilon_1 A_f + \epsilon_2 B_f|^2 \\ &= \frac{1}{1+|\epsilon_1|^2+|\epsilon_2|^2}\Big[\Sigma_f(|\epsilon_1|^2|A_f|^2 + |\epsilon_2|^2|B_f|^2) \\ &\quad + \Sigma_f(\epsilon_1 A_f)^*(\epsilon_2 B_f) + \Sigma_f(\epsilon_1 A_f)(\epsilon_2 B_f)^*\Big]\end{aligned} \tag{16}$$

Using the inequality

$$-|A|\cdot|B| \leqslant A\cdot B \leqslant |A|\cdot|B|$$

and eqs (14) and (15) in eq. (16), we get

$$\frac{[\,|\,\epsilon_1\,|\,(1+|\,\epsilon_1\,|^2)^{\frac{1}{2}}\,\Gamma_{a_1}^{\frac{1}{2}} - |\,\epsilon_2\,|\,(1+|\,\epsilon_2\,|^2)^{\frac{1}{2}}\,\Gamma_{a_2}^{\frac{1}{2}}]^2}{1+|\,\epsilon_1\,|^2+|\,\epsilon_2\,|^2}$$

$$\leqslant \Gamma a_3 \leqslant \frac{[\,|\,\epsilon_1\,|\,(1+|\,\epsilon_1\,|^2)^{\frac{1}{2}}\,\Gamma_{a_1}^{\frac{1}{2}} + |\,\epsilon_2\,|\,(1+|\,\epsilon_2\,|^2)^{\frac{1}{2}}\,\Gamma_{a_2}^{\frac{1}{2}}]^2}{1+|\,\epsilon_1\,|^2+|\,\epsilon_2\,|^2} \qquad (17)$$

which determines the limits on the magnitudes of ϵ_1 and ϵ_2. In the weak mixing situation, *i.e.*, for $|\,\epsilon_1\,|$, $|\,\epsilon_2\,| \ll 1$, eq. (17) reduces to

$$(|\,\epsilon_1\,|\,\Gamma_{a_1}^{\frac{1}{2}} - |\,\epsilon_2\,|\,\Gamma_{a_2}^{\frac{1}{2}})^2 \leqslant \Gamma a_3 \leqslant (|\,\epsilon_1\,|\,\Gamma_{a_1}^{\frac{1}{2}} + |\,\epsilon_2\,|\,\Gamma_{a_2}^{\frac{1}{2}})^2 \qquad (18)$$

3. Experimental details

The experiments were carried out using proton beam $\sim 1\mu$ A from the 1 MV Cockroft-Walton generator at this institute. Targets of NaCl and Al were prepared by vacuum evaporation onto Ta backings ($\sim 0{\cdot}5$ mm thickness). Carbon backed and self-supporting targets of Al were also used.

For the detection of α-particles plastic track detectors (cellulose nitrate) were used. Recently these detectors have proved to be of great use in the study of low α-yield reactions (Somogyi *et al* 1968, Price and Fleischer 1971, Szabo 1972). The α-particles from low yield (p, α) reactions have to be detected in the presence of elastically scattered protons whose number generally exceeds that of the α-particles by 5–6 orders of magnitude. The resultant pile up problems make the use of Si surface barrier detectors quite troublesome, especially in the case of reactions with low Q-value. This can only be mitigated by resorting to low beam currents. However this is self-defeating as the yield of the reactions are too low and statistics too poor. One would desire to use the highest beam current available both to enable detection as well as measure the cross-section for these low yield reactions.

No such problem arises in the case of plastic track detectors as we can choose the material of the plastic as well as the etching reagents in such a way as to render the detector comparatively insensitive to register proton tracks. The details of track formation and various etching techniques have been well described in the literature (Somogyi *et al* 1968, Price and Fleischer 1971, Varnagy *et al* 1974). The arrangement of the detector and targets in the scattering chamber is shown in figure 1. The target was mounted at the centre of the scattering chamber at an angle of 45° to the proton beam and the detector, shaped in the form of a rectangular cylindrical strip, was placed to cover an angular range 50°–160° in the form of an arc with the target at its centre at a distance of 10 cm from the target. A detector of this shape enables us to obtain the entire α-angular distribution in a single exposure thus eliminating normalization problems. Another target of almost identical thickness prepared along with those used for the actual measurement was mounted at the end of the scattering chamber along the direction of the beam. With the central target not in position (*see* figure 1), the beam would hit the second target. A $7{\cdot}6$ cm $\times$ $7{\cdot}6$ cm NaI (Tl) detector was used to locate the resonances in the corresponding (p, γ) reaction using the second target. After the resonance was located the central target was brought into position to inter-

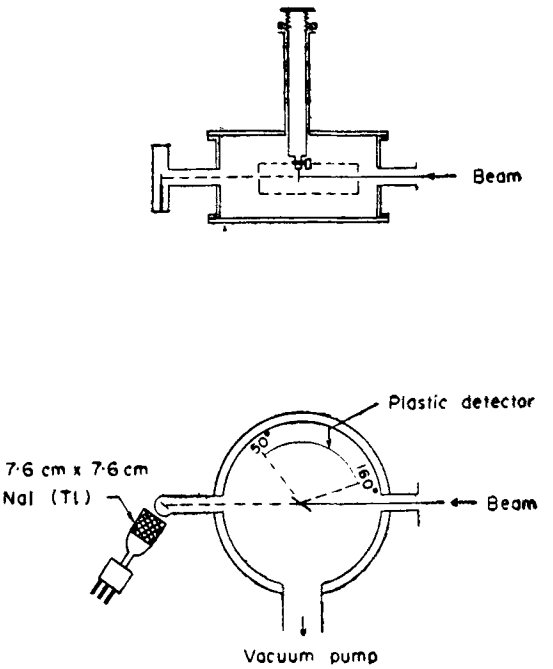

Figure 1. Arrangement of target and solid-state (plastic) track detector inside the scattering chamber, (*a*) as viewed from side (*b*) as viewed from top.

cept the beam and the α-yield on the resonance was measured. For each of the resonances studied, the yield at an energy 5 keV below the resonance energy was also measured to enable estimation of the correction for the contributions from (i) the non-resonant yield and (ii) the contaminant reactions.

After the exposure, the plastic detector was etched for 50 minutes in a solution of 150 gm NaOH + 120 gm KOH + 900 gm H_2O at 50° C. The detector was scanned under a microscope and the total number of α-tracks per cm^2 area over an angular interval of 10° was determined.

The strength of the etching solution and the period of etching were optimized by observing the α-particles arising from the decay of resonances at $E_p = 872$ keV in ^{19}F (P, α)^{16}O, at $E_p = 592$ keV in ^{23}Na(p, α) ^{20}Ne and those at $E_p = 505$ and 633 keV in ^{27}Al(p, α)^{24}Mg. Since the resonance strengths at these resonances are large and have been previously determined (Endt and Van der Leun 1967 1973) they provided good calibration of the detection system. The resonances in ^{27}Al(p, α)^{24}Mg are quite isolated and hence thick targets (thickness ≈ 10 keV at $E_p = 400$ keV) were used to measure the α-yield. In the case of ^{23}Na(p, α)^{20}Ne reaction, a thin target (thickness ≈ 1 keV at $E_p = 600$ keV) was used, since in the neighbourhood of the resonance at 739 keV in whose α-decay we are interested, there exists a strong α-decaying resonance at 744 keV.

The diameter distributions of the tracks obtained at the 505 keV resonance in ^{27}Al(p, α)^{24}Mg and at the 592 keV resonance in ^{23}Na(p, α)^{20}Ne are shown in figures 2 and 3, respectively. The distributions correspond to a single α-group in each case. The resonance strengths and the angular distribution coefficients obtained for the resonances at 505 and 633 keV in ^{27}Al(p, α)^{24}Mg are compared with those obtained in a pevious measurement (Kuperus 1963) in table 1.

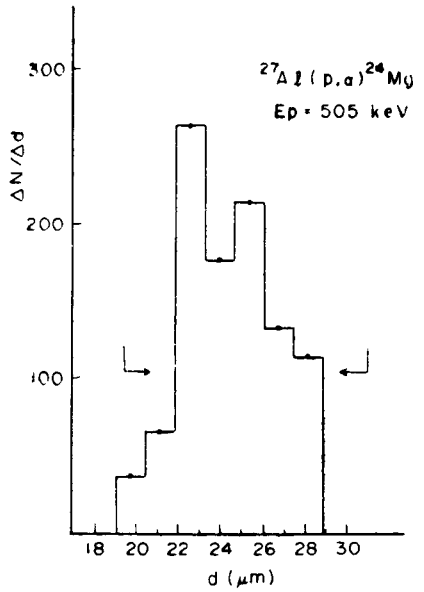

Figure 2. Distribution in the diameter of α-particle tracks at E_p = 505 keV ^{27}Al(p, α)^{24}Mg reaction. The arrows indicate the range of diameters considered for track counting.

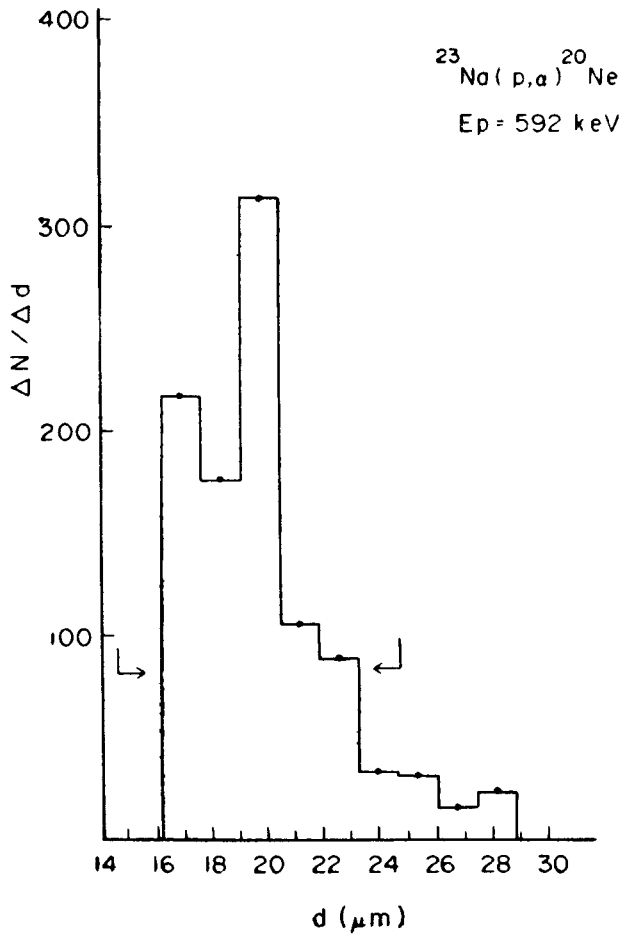

Figure 3. Distribution in the diameter of α-partcle tracks at E_p = 592 keV in ^{23}Na(p, α)^{20}Ne reaction.

Table 1. Resonance strength and angular distribution coefficients for $^{27}Al(p, \alpha)^{24}Mg$ reaction obtained in the present work compared with previous results

Resonance energy (keV)	Resonance strength $(2J+1)\,\Gamma_p\,\Gamma_\alpha/\Gamma$ (eV)		Angular distribution coefficients		
	Present work	Ku 63		Present work	Ku 63
505	1·46±0·50	1·2	a_2/a_0	0·00±0·10	0·00±0·04
			a_4/a_0	0·05±0·10	0·02±0·04
633	3·77±1·0	3·3	a_2/a_0	+0·26±0·04	+0·23±0·04
			a_4/a_0	−0·03±0·06	−0·07±0·04
			a_6/a_0	+0·04±0·07	+0·03±0·06

4. Results

4.1 *The $^{23}Na(p, \alpha)^{20}Ne$ reaction*

4.1.1. *Resonance strengths and partial widths*

The yield of α-particles was measured on the resonances at $E_p = 677$ and 739 keV and at an energy 5 keV below the corresponding resonance energies. The yields of α-particles are presented in tables 2 and 3. The angular distribution of α-particles at $E_p = 739$ keV is shown graphically in figure 4. In table 2, we find that the 'off' resonance yield is more than the 'on' resonance at $E_p = 677$ keV. This is possibly due to the contribution from the tail of the resonance at $E_p = 667$ keV in the contaminant reaction, $^{19}F(p, \alpha)^{16}O$, which has a large cross-section *viz.*, 540 mb as against few μb in case of ^{23}Na. The sources of flourine contamination are (i) the Ta backing itself and (ii) the oil vapour from the diffusion pumps The contribution from the second source can be minimised using liquid nitrogen traps. A quantitative estimate of the amount of ^{19}F present is difficult since the amount of ^{19}F keeps increasing with time due to deposition of oil vapour. We thus cannot obtain a reliable value for the resonance strength of this resonance. However we can set an upper limit of 3.3×10^{-3} eV for the value of resonance strength, $(2J+1)\,\Gamma_p\,\Gamma\alpha/\Gamma$.

The slight asymmetries observed about 90° in the angular distribution of both the 'on' and 'off' resonance yields at $E_p = 739$ keV possibly arise due to interference with the resonance at 744 keV. The difference between the 'on' and 'off' resonance yields, which corresponds to the yield of the resonance, however, is almost isotropic. The value for the resonance strength $(2J+1)\,\Gamma_p\,\Gamma\alpha/\Gamma$ obtained for this resonance by comparing its yield to that of the resonance at $E_p = 592$ keV is $(1{\cdot}47 \pm 0{\cdot}5)$ eV.

Since the resonances have $J^\pi = 3^+$, they cannot be excited as resonances in $^{20}Ne(\alpha, \gamma)^{24}Mg$ reaction and thus the strength of the (α, γ) reaction is not available. To deduce the partial α-widths, we assume $\Gamma_p \approx \Gamma$. If this assumption is incorrect, the widths obtained give the lower limits for the α-widths. The

Table 2. Number of α-tracks detected *versus* observation angle from ^{23}Na $(p, \alpha)^{20}$Ne reaction at $E_p = 677$ keV. Area of detector = 25 mm^2. Total proton charge incident on the target during the exposure = 0·02 Coulomb.

Angle in degrees	Number of α-tracks		
	'On' resonance	'Off' resonance	Difference ('On'–'Off')
50–60	116	152	− 36
60–70	172	187	− 15
70–80	121	201	− 80
80–90	159	200	− 41
90–100	196	291	− 95
100–110	232	335	−103
110–120	253	230	+ 23
120–130	180	315	−135
130–140	176	294	−118
140–150	159	225	− 66
150–160	154	180	− 26

Table 3. Number of α-tracks detected *versus* observation angle from ^{23}Na $(p, \alpha)^{20}$Ne reaction at $E_p = 739$ keV. Area of detector = 100 mm^2. Total proton charge incident on the target during the exposure = 0·01 Coulomb.

Angle in degrees	Number of α-tracks		
	'On' resonance	'Off' resonance	Difference ('On'–'Off')
60–70	3748	2896	852
70–80	3659	2809	850
80–90	3602	2707	895
90–100	3495	2750	745
100–110	3542	2640	902
110–120	3251	2404	847
120–130	3007	2162	845
130–140	2792	1780	1012
140–150	2327	1558	769
150–160	2061	1259	802

widths deduced under this assumption are presented in table 4. The dimensionless reduced α-widths were obtained from the observed widths by incorporating the effect of penetrability and dividing by the Wigner limit $3\hbar^2/2\mu R^2$. The penetrabilities were calculated using the fromalism of Sharp *et al* (1955), with the

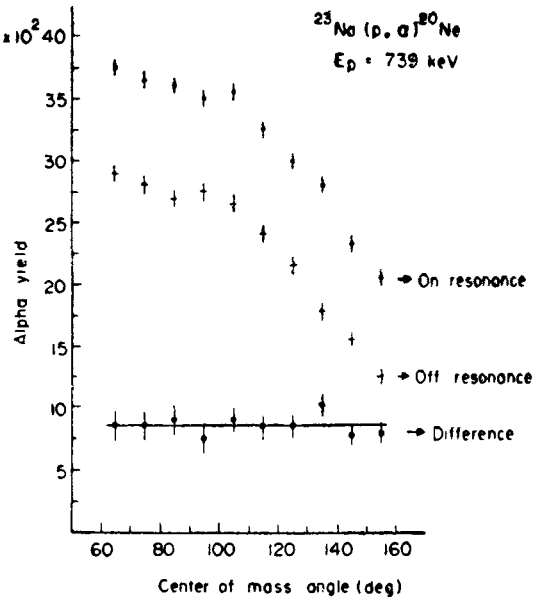

Figure 4. Angular distribution of α-particles obtained at "On", and "Off" resonance at $E_p = 739$ keV in ^{23}Na $(p, \alpha)^{20}$Ne reaction. The ordinate represents actual number of α-tracks registered per cm^2 area of the detector.

Table 4. Partial and reduced α-widths for resonances in ^{23}Na(p, α)^{20}Ne reaction. The widths are deduced under the assumption $\Gamma_p \approx \Gamma$.

E_x (^{24}Mg) (MeV)	E_p (keV)	J^π	$(2J+1)\,\Gamma_\alpha$ (eV)	Γ_α (eV)	θ_α^2
12·342	677	3+	$\leqslant 3{\cdot}4\times10^{-3}$	$0{\cdot}5\times10^{-3}$	$4{\cdot}6\times10^{-4}$
12·402	739	3+	$1{\cdot}5\pm0{\cdot}5$	$0{\cdot}21\pm0{\cdot}07$	0·11

interaction radius given by $R = r_0$ (fm) $(A^{\frac{1}{3}} + m^{\frac{1}{3}})$ where A and m are the mass number of the target and projectile respectively and $r_0 = 1{\cdot}4$ fm. The values obtained for the penetrabitities and hence the reduced widths depend very much on the value of r_0 chosen, specially at low projectile energies below the Coulomb barrier. However, as can be seen from table 5. the ratio of penetrabilities at two different energies does not depend sensitively on the choice of r_0.

4.1.2. *Coulomb matrix element*

Using the values for the reduced α-widths [from table 4 and eq. (6)], the value of the mixing parameter,

$$|\epsilon|^2 = \frac{4{\cdot}6 \times 10^{-4}}{0{\cdot}11} = 4{\cdot}18 \times 10^{-3}$$

or

$$|\epsilon| = 0{\cdot}065$$

is obtained.

Table 5. Comparison of proton and alpha particle penetrabilities calculated using different values for the interaction radius, R, defined by $R = r_0(A^{1/3} + m^{1/3})$ in fm.

(*a*) System: $^{23}Na + p$

E_p (MeV)	l_p	$P_{lp} = 2\rho/A_{lp}^2$	
		$r_0 = 1{\cdot}2$	$r_0 = 1{\cdot}4$
0·592	1	$4{\cdot}82\times10^{-4}$	$1{\cdot}01\times10^{-3}$
0·677	2	$7{\cdot}43\times10^{-5}$	$1{\cdot}92\times10^{-4}$
0·739	2	$1{\cdot}37\times10^{-4}$	$3{\cdot}53\times10^{-4}$
$P_2(0{\cdot}739)/P_2(0{\cdot}677) =$		1·84	1·84

(*b*) System: $^{20}Ne + \alpha$ at resonances in $^{23}Na + p$ reaction

E_p (MeV)	E_α (MeV)	l_α	$P_{l\alpha} = 2\rho/A_{l\alpha}^2$	
			$r_0 = 1{\cdot}2$	$r_0 = 1{\cdot}4$
0·592	2·944	3	$2{\cdot}58\times10^{-3}$	$1{\cdot}17\times10^{-2}$
0·677	1·395	2	$4{\cdot}40\times10^{-7}$	$2{\cdot}20\times10^{-6}$
0·739	1·454	2	$8{\cdot}57\times10^{-7}$	$4{\cdot}27\times10^{-6}$
$P_2(0{\cdot}739)/P_2(0{\cdot}677) =$			1·95	1·94

Upper limits of 90 and 70 eV have been set for the widths of the resonances at 739 and 677 keV (Wagner and Heitzmann 1960). Then using eq. (3)

$$|\eta_1 - \eta_2| \simeq E_1 - E_2 = 739 - 677 = 62 \text{ keV}$$

and the Coulomb matrix element, given by eq. (7), is

$$\langle \psi(T_<) \mid H_e \mid \psi(T_>) \rangle = 4{\cdot}01 \text{ keV}.$$

4.2. *The* $^{27}Al(p, \alpha)^{24}Mg$ *reaction*

4.2.1. *Resonance strengths and partial widths*

The yield of α-particles on the 295, 327 and 405 keV resonances and at energies 5 keV below the respective resonance energies measured using a thick target are presented in tables 6 to 8. From table 7, we find that there is no observable α-yield from the resonance at $E_p = 327$ keV. The deduced resonance strengths and the angular distribution coefficients are presented in table 9. The low yields of the reaction result in large statistical errors on measurement which reflect as large errors on the angular distribution coefficients. Not much significance can thus be attributed to the values of the angular distribution coefficients.

The compound states in ^{28}Si excited through the $^{27}Al(p, \gamma)^{28}Si$ reaction as resonances at $E_p = 327$ and 405 keV have been observed to be excited in $^{24}Mg(\alpha, \gamma)^{28}Si$ reaction as well (Smulders and Endt 1962). No resonance is observed in the latter reaction at α-energies corresponding to the resonance at $E_p = 295$ keV. However, from the excitation function presented for the (α, γ) reaction (Smulders and Endt 1962) it is possible to place an upper limit on the resonance

Table 6. Number of α-tracks detected *versus* observation angle from $^{27}Al(p, \alpha)^{24}Mg$ reaction at $E_p = 295$ keV. Area of detector = 100 mm². Total proton charge incident on the target during the exposure = 0·01 Coulomb.

Angle in degrees	Number of α-tracks		
	'On' resonance	'Off' resonance	Difference ('On'−'Off')
60–70	682	550	132
70–80	700	564	136
80–90	677	565	112
90–100	637	560	67
100–110	726	583	143
110–120	713	564	149
120–130	684	556	128
130–140	662	555	107
140–150	674	583	91
150–160	629	575	54

Table 7. Number of α-tracks detected *versus* observation angle from $^{27}Al(p, \alpha)^{24}Mg$ reaction at $E_p = 327$ keV. Area of detector = 32 mm². Total proton charge incident on the target during the exposure = 0·055 Coulomb.

Angle in degrees	Number of α-tracks		
	'On' resonance	'Off' resonance	Difference ('On'−'Off')
50–60	965	1057	−92
60–70	897	945	−48
70–80	955	942	+13
0–90	965	960	+ 5
90–100	1048	1021	+27
100–110	1019	1008	+11
110–120	1071	1131	−60
120–130	1075	1149	−74
130–140	1108	1025	+83
140–150	1198	1240	−42

strength for the (α, γ) reaction. Since, we have a knowledge of the strengths of the (p, γ), (p, α) and (α, γ) reactions leading to the same compound states in ^{28}Si, the partial widths Γ_p, Γ_γ and Γ_α can all be determined. The partial and the reduced widths are presented in tables 10 and 11. The particle penetrabilities were calculated as detailed earlier in section 4.1.1.

4.2.2 *Coulomb matrix elements*

Since we have here a case of an IAR splitting into three components, as discussed in section 2, the Coulomb matrix elements responsible for the mixing cannot be

Table 8. Number of α-tracks detected *versus* observation angle from $^{27}Al(p, \alpha)^{24}Mg$ reaction at $E_p = 405$ keV. Area of detector = 25mm². Total proton charge incident on the target during the exposure = 0·04 Coulomb.

Angle in degrees	Number of α-tracks		
	'On' resonance	'Off' resonance	Difference ('On'−'Off')
50–60	1252	939	313
60–70	1205	904	301
70–80	1338	934	404
80–90	1237	934	304
90–100	1194	949	245
100–110	1276	931	345
110–120	1440	1010	430
120–130	1311	1008	303
130–140	1268	1046	222
140–150	1264	1026	238

Table 9. Resonance strengths and angular distribution coefficients for ^{27}Al $(p, \alpha)^{24}Mg$ reaction. The angular distribution coefficients are obtained from least square fitting to the data.

Resonance energy (keV)	Resonance strength $(2J+1)\frac{\Gamma_p \Gamma_\alpha}{\Gamma}$ (eV)	Angular distributon coefficients normalised with respect to a_0	
		a_2	$-0{\cdot}34\pm0{\cdot}24$
295	$(26\pm9)\times10^{-3}$	a_4	$-0{\cdot}27\pm0{\cdot}30$
		a_6	$-0{\cdot}60\pm0{\cdot}41$
327	$\leqslant 1{\cdot}4\times10^{-3}$		
		a_2	$0{\cdot}25\pm0{\cdot}34$
405	$(64\pm20)\times10^{-3}$	a_4	$0{\cdot}55\pm0{\cdot}38$
		a_6	$0{\cdot}65\pm0{\cdot}49$

Table 10. Resonance strengths and cross-sections for the $^{27}Al(p, \alpha)^{24}Mg$ reaction

Resonance energy (keV)	E_x (^{28}Si) (MeV)	J^π	Resonance strengths in eV			Resonance cross-sesion in barns		
			(p, α)	(p, γ)*	(α, γ)†	$\sigma_{p\gamma}$	$\sigma_{p\alpha}$	$\sigma_{\alpha\gamma}$
295	11·869	4^+	$0{\cdot}026\pm0{\cdot}009$	0·0042	0·002	0·22	1·55	0·05
327	11·898	4^+	$\leqslant 0{\cdot}0014$	0·028	0·035	0·21	0·01	0·49
405	11·974	4^+	$0{\cdot}064\pm0{\cdot}020$	0·150	0·070	0·83	0·59	0·92

* From (Endt 1967, 1974).
† From (Smulders 1962).

Table 11. Widths, partial widths and dimensionless reduced particle widths of resonance levels in ^{28}Si.

E_x (^{28}Si) (MeV)	E_p (keV)	J^π	Γ (meV)	Γ_p (meV)	Γ_α (meV)	Γ_γ (meV)	θ_p^2 ($\times 10^{-3}$)	θ_α^2 ($\times 10^{-3}$)
11·869	295	4^+	14·7	9·5	4·5	0·7	20·0	6·8
11·898	327	4^+	95·2	3·4	4·2	87·6	2·2	4·8
11·974	405	4^+	100·0	39·0	18·2	42·8	2·5	11·0

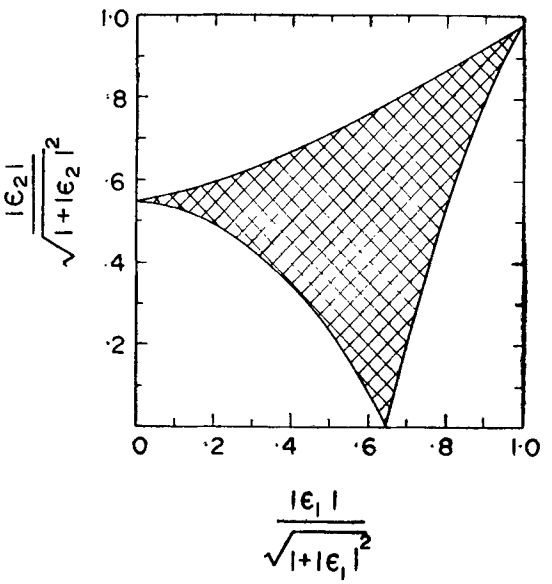

Figure 5. Plot of the normalised mixing parameter $|\epsilon_1|/\sqrt{1+|\epsilon_1|^2}$ *versus* $|\epsilon_2|/\sqrt{1+|\epsilon_2|^2}$ for three level mixing in ^{28}Si. The region under the shaded portion is allowed by the limits obtained from eq. (17).

determined. We use the eq. (17) and the reduced α-widths from table 11 to determine the bounds on the mixing parameters. The result is shown graphically in figure 5. The normalised parameters $|\epsilon_i|/\sqrt{1+|\epsilon_i|^2}$ are chosen for ease of presentation. From the figure, we find that very small values for both $|\epsilon_1|$ and $|\epsilon_2|$ are excluded. However, both $|\epsilon_1|$ and $|\epsilon_2|$ could simultaneously be very large, but that situation would correspond to two IAS mixing with one state of lower isospin. The corresponding limits on the Coulomb matrix elements in ^{28}Si, calculated using eq. (7), are

$$\langle \psi(T_<) \mid H_c \mid \psi(T_>) \rangle \leqslant 16 \text{ keV}$$

and

$$\langle \psi'(T_<) \mid H_c \mid \psi(T_>) \rangle \leqslant 39 \text{ keV}.$$

5. Discussion

The observed α-decay of the IAR's indicate the presence of isospin mixing. For

the nucleus, ^{24}Mg, the mixing is found to be quite weak as indicated by the small value of the mixing parameter, ϵ. However, in the case of ^{28}Si, the situation is different and we can definitely rule out the situation of very weak mixing as indicated by the limits on the mixing parameters. Although in both nuclei, the region of excitation is around 12 MeV, the observed mixing strengths are quite different. Further understanding of the mixing phenomenon would very much depend on the knowledge of the structure of the states at these high excitations.

In the nucleus ^{28}Si, we find that the reduced proton and α-widths are of the same order of magnitude in terms of the Wigner limits (*i.e.*, single particle units). This suggests that the probability of the configuration in ^{28}Si with an alpha particle at the nuclear surface is nearly the same as the probability for the configuration with a proton outside the corresponding residual nucleus (^{27}Al).

Acknowledgements

We thank S. K. Bhattacherjee for evincing keen interest and providing constant encouragement throughout the course of this work. Our thanks are due to C V K Baba and C S Warke for many illuminating discussions and useful suggestions with regard to analysis of data. We also thank B M Bellara and V V Samant for having assisted us in the scanning of the plastic track detectors.

References

Endt P M and Van der Leun C 1967 *Nucl. Phys.* **A105** 1
Endt P M and Van der Leun C 1973 *Nucl. Phys.* **A214** 1
Kuperus J, Glaudemans P W M and Endt P M 1963 *Physica* **29** 1281
Meyer M A and Wolmarans N S 1969 *Nucl. Phys.* **A136** 663
Meyer M A, Reinecke J P L and Reitmann D 1972 *Nucl. Phys.* **A185** 625
McDonald W M 1960 *Nucl. Spectroscopy* Part B, ed. F Ajzenberg Selove (Academic Press, New York) p 940
Price P B and Fleischer R L 1971 *Ann. Rev. Nucl. Sci.* **21** 295
Radicati L A 1953 *Proc. Phys. Soc.* (London) **A66** 139
Shanley P E 1975 *Phys. Rev. Lett.* **34** 218
Sharp W T, Gove H E and Paul E B 1955 *Graphs of Coulomb Functions*, Atomic Energy of Canada Report No. AECL-268
Smulders P J M and Endt P M 1962 *Physica* **28** 1093
Somogyi G, Schlenk B, Varnagy M, Masko L and Valek A 1968 *Nucl. Instrum. Methods* **63** 189
Szabö J, Csikai J and Varnagy M 1972 *Nucl. Phys.* **A195** 527
Varnagy M, Csikai J, Szabö J, Szegedi S and Banhalmi J 1974 *Nucl. Instrum. Methods* **119** 451
Wagner Von S and Heitzmann M 1960 *Z. Nature* **15A** 74
Warke C S 1975 Private Communication, to be published.